Preparation and study dielectric properties of Copper-nickel ferrite nanoparticles by hydrothermal method

Farah T. M. Noori

Department of physics, College of science, University of Baghdad

Corresponding author email:farah.noori@scbaghdad.edu.iq

Alternative e-mail:farah_t258@yahoo.com

Received 13 January 2015 ; Accepted 15 February 2015

Abstract

Copper-nickel ferrites were synthesized by employing hydrothermal sol gel technique with general formula $Ni_{1-x}Cu_xFe_2O_4$where x=0.0, 0.3 and 0.5. The pellets of 1.5 cm diameter were prepared with 2 mm thickness by applying pressure of 3 Tons and then sintering with different temperature (600, 700, 800 and 900) °C for further characterization. The main cubic spinal structure phase for all samples was confirmed by x-ray diffraction patterns The prepared specimens were characterized by XRD structural analysis indicates that the percentage of iron ions in B site increases, the intensity of the (311) peak increases. This indicates that the structural changes of the $Ni_{1-x}Cu_xFe_2O_4$, arise from the shifting of ions between A and B sites. Atomic force microscopy showed that the average grain size was about 52.3nm. The morphology was studies using SEM and it is found that the grains had an irregular distribution and irregular shape. The Copper-nickel ferrite ($Ni_{1-x}Cu_xFe_2O_4$) shows high σac conductivity due to dipole polarization. The dielectric constants of the sampleswere noticed to decrease with frequency and Cu addition and due to the different sintering temperatures.

Key words: Copper-nickel ferrite, hydrothermal technique, Ac conductivity, dielectric constants.

Preparation and study dielectric properties of Copper-nickel ferrite nanoparticles by hydrothermal method

Farah T. M. Noori

تحضير ودراسة الخصائص العزلية لنانوي نحاس-نيكل فرايت بتقنية الحرارية المائية

فرح طارق محمد نوري

قسم الفيزياء / كلية العلوم / جامعة بغداد

الخلاصة

تم تحضير نيكل فرايت بتقنية الحرارية المائية – sol gel ذو الصيغة التركيبية $Ni_{1-x}Cu_xFe_2O_4$ حيث ان x=0.3, 0.5 تم اعداد الاقراص ذات القطر 1.5cm بسمك 2 mm بضغط مسلط 3 ton ثم التلبيد بدرجات حرارة مختلفة (600, 700, 800 and 900) °C لغرض التشخيص. طور التركيب الرئيسي لكل العينات السبينل المكعب الذي شخص باستخدام حيود الاشعة السينية وكذلك التحليل البنيوي لكل العينات تم تشخيصها بالاشعة السينية ان نسبة الحديد تزداد بالموقع B عند معامل ميلر (311) وهذا يدل على ان التغييرات الهيكلية ل $Ni_{1-x}Cu_xFe_2O_4$ ، تنشأ من التحول من الأيونات بين المواقع A و B. أظهر مجهر القوة الذرية أن متوسط حجم الحبوب بلغ نحو 52.3nm. صور المجهر الالكتروني بينت ان الحبيبات غير منتظمة التوزيع والشكل. التوصيلية الكهربائية تزداد بزيادة تركيز النحاس وبزيادة درجة حرارة التلبيد. ثوابت العزل تنخفض مع زيادة تركيز النحاس والتردد وكذلك بسبب اختلاف درجات الحرارة للتلبيد.

الكلمات المفتاحية: نحاس-نيكل فرايت ، التقنية الحرارية المائية ، التوصيلية الكهربائية المتناوبة وثوابت العزل

Introduction

Spinel is the most widely used family of ferrites. High values of electrical resistivity and low eddy current losses make them ideal for their use at microwave frequenciesSpinel ferrite nanoparticles, a sort of delicate attractive materials with structural recipe of MFe_2O_4 (M =divalent metal particle, e.g. Mn, Mg, Zn, Ni, Co, Cu, and so on).They are attractive because of their numerous specialized applications importance in ferro fluids, magnetic drug delivery, nano gadgets, sensors and hyper-thermic for cancer treatment [1,2].

electrical and attractive properties of ferrites on the way of the particles, their charges and their dissemination among tetrahedral (A) and octahedral (B) destinations [3]. Nickel ferrite is one of the adaptable and mechanically vital delicate ferrite materials as a result of its ordinary ferromagnetic properties, low conductivity and therefore lower swirl current misfortunes, high electrochemical strength, synergist conduct, plenitude in nature, etc[4]. This ferrite is it crystallizes in inverse spinel structure i.e. tetrahedral sites are occupied by ferric ions and the octahedral sites by ferric and nickel [5, 6].

Experimental

Nanoparticles of copper substituted nickel ferrites with the general formula $Ni_{1-x}Cu_xFe_2O_4$ (where x=0.0, 0.3 and 0.5) were prepared using hydro thermal sol-gel method). In this method each sample was prepared by taking the desired proportion of precursor nitrates., nickel nitrate$Ni(NO_3)_2.6H_2O$, iron nitrate $Fe(NO_3).9H_2O$ and copper nitrate $Cu(NO_3).4H_2O$.The precursorswere separately dissolved in minimum amount of water. After heating them at 80-90°C all the solutions were mixed. The solution obtained was stirred for mention the time in minuetsand then mixed with methanol alcohol and KaOH homogenously after till gel formationThis gel self-ignites and results in nano particles of desired ferritethat the powderwill wishing with distill water. The solution was again stirred.Finally, AFM was performed to measure the average diameter and the grain size for fine graded nickel ferrite particles are formedby using AA3000 scanning probe Microscopy by Angstrom Advanced Inc (USA).

. The pellets of 1.5 cm diameter are prepared with 2 mm thickness by applying pressure of 3 Tons and then sintering with different temperature (600, 700, 800 and 900)°Cfor further characterization. The pellets are coated with silver paste on both sides of the surfaces to obtain better contacts. X-ray diffraction patterns of $Ni_{1-x}Cu_xFe_2O_4$ series samples were obtained over the 2θ range of 10-60o, using Philips X' Pert analytical diffractmeter with CuKα1 radiation. The morphological features of the samples were studied using a JEOL JSM-840 Scanning Electron Microscope.

Result and Discussion

1-The atomic force microscopy

The atomic force microscopy of $NiFe_2O_4$ powderferrites (where x=0.0) showed that the average grain size was 53.83nm as shown in figure.1. On the other hand the average roughness increases from 1.83nm.

Diameter(nm) <	Volume(%)	Cumulation(%)	Diameter(nm) <	Volume(%)	Cumulation(%)	Diameter(nm) <	Volume(%)	Cumulation(%)
10.00	0.75	0.75	35.00	4.48	8.96	60.00	11.19	61.94
15.00	0.75	1.49	40.00	5.97	14.93	65.00	8.96	70.90
20.00	0.75	2.24	45.00	8.21	23.13	70.00	17.16	88.06
25.00	1.49	3.73	50.00	16.42	39.55	75.00	11.94	100.00
30.00	0.75	4.48	55.00	11.19	50.75			

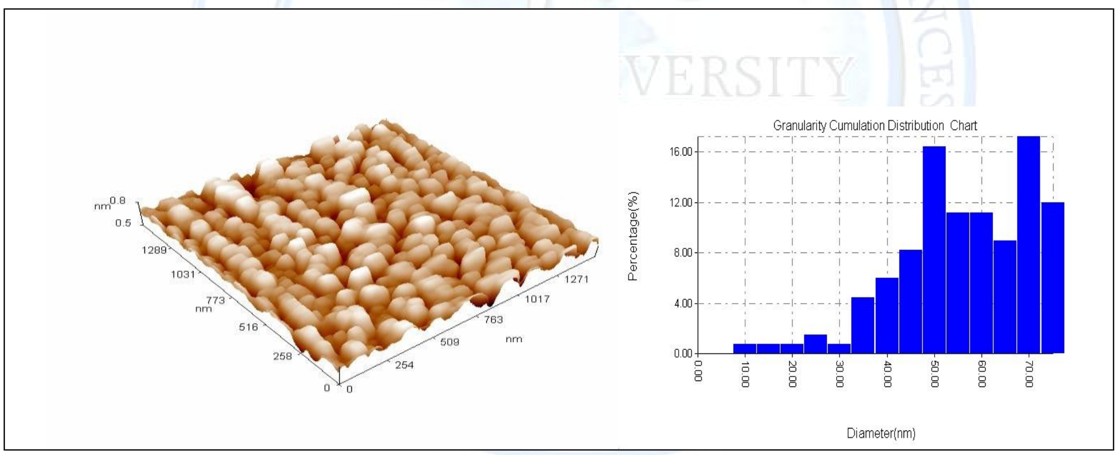

Fig.1: AFM micrographs for the composition $Ni_{1-x}Cu_xFe_2O_4$

2-X-Ray Diffraction

The x-ray diffraction patterns for Copper addition nickel ferrite $Ni_{1-x}Cu_xFe_2O_4$ with (x=0.3,0.5) sintered at 600, 700 800 and 900 °C for (2 h) are shown in Fig.2 and Fig.3 respectively.

All the XRD spectra of samples show good crystallization, with well-defined diffraction lineswhichindicate the formation of crystalline cubic spinel phase ferrite with space group (*Fd3m*)[7]. The samples produced six well defined diffraction peaks. The presence of the strong diffraction peaks corresponding to the planes (220), (311), (222), (400), (422) and (333) indicates the presence of cubic spinel phase. The peaks showed different amounts of crystallinity depending upon additions rate of Cu^{+3} and intensity of this peak increases with the increase of sintering 600, 700, 800 and 900°C temperature.

It can be noticed from the x-ray patterns that the peaks at (2θ=35.87° and43.6°) referred to (311) and (400) plane directions, respectively. With that the strongest peak occurs for the (311) plane at 2θ=35.87°. A point of interest is that the preferential orientation is the (311) direction. Miller indices (hkl) and interplaner spacing (d_{hkl}) for $Ni_{1-x}Cu_xFe_2O_4$ ferrites are listed in tables(1) and (2) respectively.

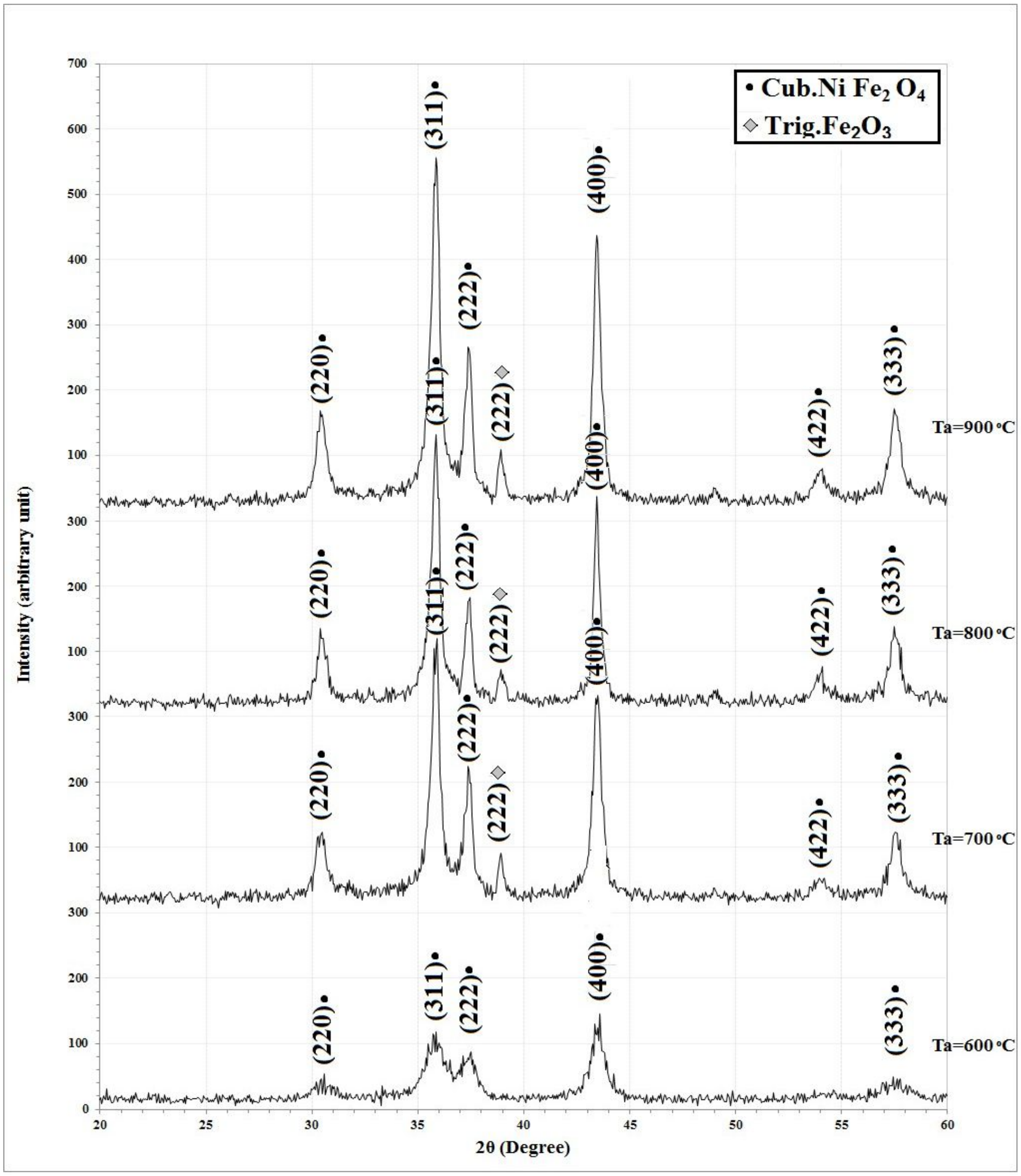

Fig.2: X-ray diffraction patterns for bulk $Ni_{0.7}Cu_{0.3}Fe_2O_4$ ferrites with different sintering temperatures.

Table 1: X-ray diffraction pattern data for bulk $Ni_{0.7}Cu_{0.3}Fe_2O_4$ ferrites with different sintering temperatures.

Ta (C)	2θ (Deg.)	FWHM (Deg.)	d_{hkl} Exp.(Å)	G.S (nm)	d_{hkl} Std.(Å)	hkl	phase	card No.
600	30.5536	0.7953	2.9235	10.4	2.9486	(220)	Cub.$NiFe_2O_4$	96-591-0065
	35.8775	1.0191	2.5010	8.2	2.5146	(311)	Cub.$NiFe_2O_4$	96-591-0065
	37.4794	1.1932	2.3977	7.0	2.4076	(222)	Cub.$NiFe_2O_4$	96-591-0065
	43.6042	0.5871	2.0740	14.6	2.0850	(400)	Cub.$NiFe_2O_4$	96-591-0065
	57.5501	1.3095	1.6002	6.9	1.6050	(333)	Cub.$NiFe_2O_4$	96-591-0065
700	30.5065	0.5179	2.9279	15.9	2.9486	(220)	Cub.$NiFe_2O_4$	96-591-0065
	35.8775	0.3981	2.5010	21.0	2.5146	(311)	Cub.$NiFe_2O_4$	96-591-0065
	37.3852	0.3607	2.4035	23.3	2.4076	(222)	Cub.$NiFe_2O_4$	96-591-0065
	38.8928	0.1808	2.3137	46.6	2.2938	(222)	Trig.Fe_2O_3	96-101-1268
	43.4629	0.4536	2.0804	18.9	2.0850	(400)	Cub.$NiFe_2O_4$	96-591-0065
	54.0165	0.8323	1.6963	10.7	1.7024	(422)	Cub.$NiFe_2O_4$	96-591-0065
	57.5972	0.6695	1.5990	13.5	1.6050	(333)	Cub.$NiFe_2O_4$	96-591-0065
800	30.4122	0.4678	2.9368	17.6	2.9486	(220)	Cub.$NiFe_2O_4$	96-591-0065
	35.8775	0.4003	2.5010	20.9	2.5146	(311)	Cub.$NiFe_2O_4$	96-591-0065
	37.4794	0.3095	2.3977	27.1	2.4076	(222)	Cub.$NiFe_2O_4$	96-591-0065
	38.9399	0.3594	2.3110	23.4	2.2938	(222)	Trig.Fe_2O_3	96-101-1268
	43.4629	0.2961	2.0804	28.9	2.0850	(400)	Cub.$NiFe_2O_4$	96-591-0065
	54.0636	0.5725	1.6949	15.6	1.7024	(422)	Cub.$NiFe_2O_4$	96-591-0065
	57.5029	0.3576	1.6014	25.3	1.6050	(333)	Cub.$NiFe_2O_4$	96-591-0065
900	30.4122	0.4257	2.9368	19.3	2.9486	(220)	Cub.$NiFe_2O_4$	96-591-0065
	35.8775	0.3643	2.5010	22.9	2.5146	(311)	Cub.$NiFe_2O_4$	96-591-0065
	37.3852	0.2816	2.4035	29.8	2.4076	(222)	Cub.$NiFe_2O_4$	96-591-0065
	38.8928	0.3271	2.3137	25.8	2.2938	(222)	Trig.Fe_2O_3	96-101-1268
	43.4629	0.2695	2.0804	31.7	2.0850	(400)	Cub.$NiFe_2O_4$	96-591-0065
	54.0636	0.5210	1.6949	17.1	1.7024	(422)	Cub.$NiFe_2O_4$	96-591-0065
	57.5029	0.3254	1.6014	27.8	1.6050	(333)	Cub.$NiFe_2O_4$	96-591-0065

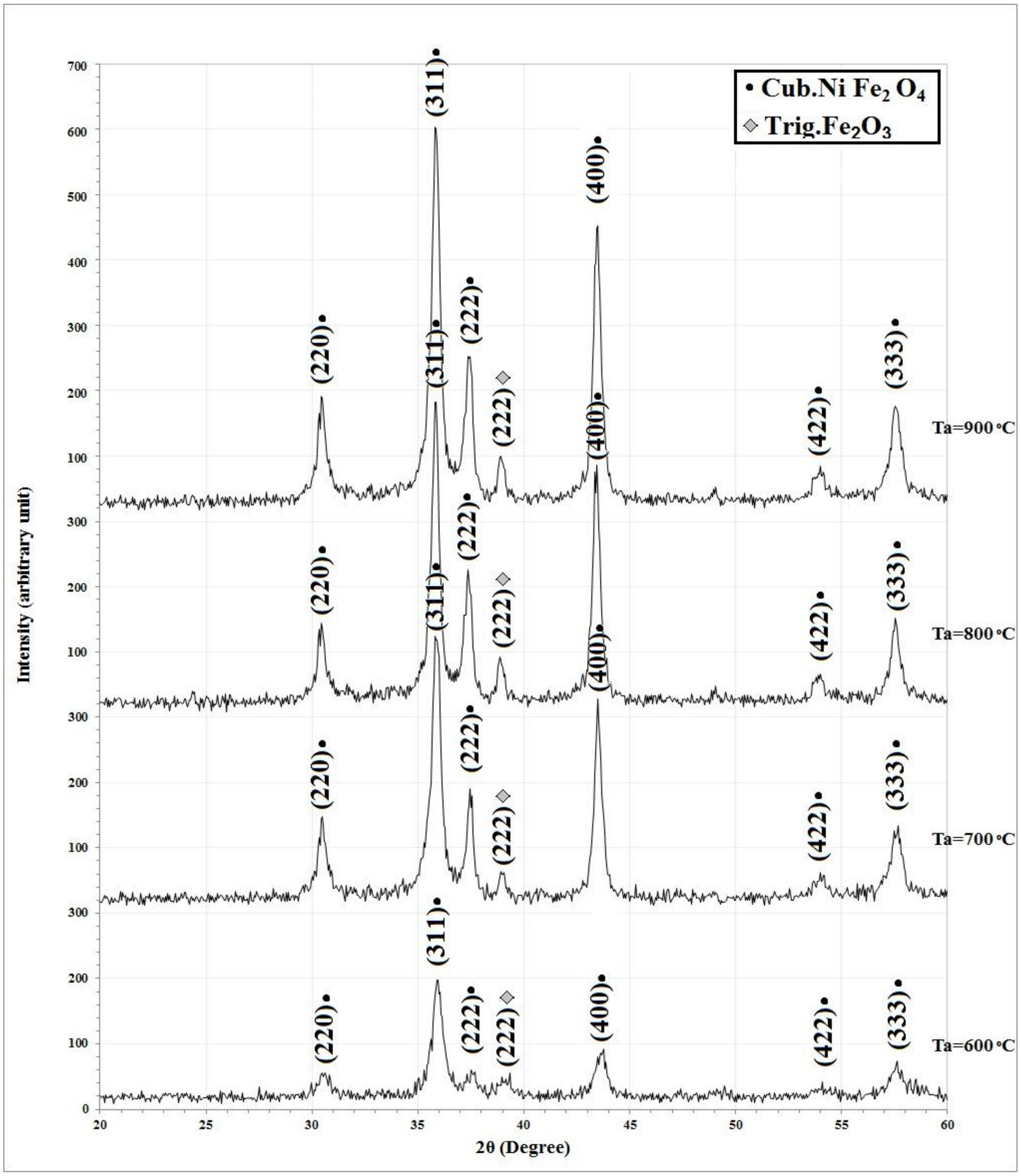

Fig.3: X-ray diffraction patterns for bulk $Ni_{0.5}Cu_{0.5}Fe_2O_4$ ferrites with different sintering temperature.

Table 3: X-ray diffraction pattern data for bulk $Ni_{0.5}Cu_{0.5}Fe_2O_4$ ferrites with different sintering temperature.

Ta (°C)	2θ (Deg.)	FWHM (Deg.)	d_{hkl} Exp.(Å)	G.S (nm)	d_{hkl} Std.(Å)	hkl	phase	card No.
600	30.5536	0.8071	2.9235	10.2	2.9486	(220)	Cub.$NiFe_2O_4$	96-591-0065
	35.9717	0.5774	2.4946	14.5	2.5146	(311)	Cub.$NiFe_2O_4$	96-591-0065
	37.6207	1.2217	2.3890	6.9	2.4076	(222)	Cub.$NiFe_2O_4$	96-591-0065
	39.2697	0.7833	2.2924	10.8	2.2938	(222)	Trig.Fe_2O_3	96-101-1268
	43.7927	0.5819	2.0655	14.7	2.0850	(400)	Cub.$NiFe_2O_4$	96-591-0065
	54.1578	0.3478	1.6922	25.7	1.7024	(422)	Cub.$NiFe_2O_4$	96-591-0065
	57.6443	0.7333	1.5978	12.4	1.6050	(333)	Cub.$NiFe_2O_4$	96-591-0065
700	30.5536	0.3840	2.9235	21.4	2.9486	(220)	Cub.$NiFe_2O_4$	96-591-0065
	35.8775	0.4494	2.5010	18.6	2.5146	(311)	Cub.$NiFe_2O_4$	96-591-0065
	37.4794	0.3072	2.3977	27.3	2.4076	(222)	Cub.$NiFe_2O_4$	96-591-0065
	38.9870	0.4362	2.3084	19.3	2.2938	(222)	Trig.Fe_2O_3	96-101-1268
	43.5100	0.3284	2.0783	26.0	2.0850	(400)	Cub.$NiFe_2O_4$	96-591-0065
	53.9694	0.8394	1.6976	10.6	1.7024	(422)	Cub.$NiFe_2O_4$	96-591-0065
	57.6443	0.5474	1.5978	16.6	1.6050	(333)	Cub.$NiFe_2O_4$	96-591-0065
800	30.5065	0.3659	2.9279	22.5	2.9486	(220)	Cub.$NiFe_2O_4$	96-591-0065
	35.8775	0.3685	2.5010	22.7	2.5146	(311)	Cub.$NiFe_2O_4$	96-591-0065
	37.4323	0.3578	2.4006	23.4	2.4076	(222)	Cub.$NiFe_2O_4$	96-591-0065
	38.8928	0.3003	2.3137	28.1	2.2938	(222)	Trig.Fe_2O_3	96-101-1268
	43.4158	0.3825	2.0826	22.4	2.0850	(400)	Cub.$NiFe_2O_4$	96-591-0065
	53.9694	0.7478	1.6976	11.9	1.7024	(422)	Cub.$NiFe_2O_4$	96-591-0065
	57.5501	0.3827	1.6002	23.7	1.6050	(333)	Cub.$NiFe_2O_4$	96-591-0065
900	30.5065	0.3330	2.9279	24.7	2.9486	(220)	Cub.$NiFe_2O_4$	96-591-0065
	35.8775	0.3353	2.5010	24.9	2.5146	(311)	Cub.$NiFe_2O_4$	96-591-0065
	37.4323	0.3256	2.4006	25.8	2.4076	(222)	Cub.$NiFe_2O_4$	96-591-0065
	38.9399	0.2733	2.3110	30.8	2.2938	(222)	Trig.Fe_2O_3	96-101-1268
	43.5100	0.3481	2.0783	24.6	2.0850	(400)	Cub.$NiFe_2O_4$	96-591-0065
	54.0165	0.6805	1.6963	13.1	1.7024	(422)	Cub.$NiFe_2O_4$	96-591-0065
	57.5501	0.3483	1.6002	26.0	1.6050	(333)	Cub.$NiFe_2O_4$	96-591-0065

The X-ray densities (dx) for all the sintering samples are tabulated in table 4 which was calculated using the equation dx = 8M/Na,3 where M is the molecular mass of the sample, N is Avogadro's number and 'a' is the lattice parameter[4]. It is clearly that the X-ray density increases linearly with increasing copper con- centration which can be attributed to the heavier concentration of copper atom as compared to that of nickel atom.

Table 4: X-ray density for bulk $Ni_{1-x}Cu_xFe_2O_4$ ferrites with 600°Csintering temperature.

X	d_{hkl}(A)	(hkl)	M(g/mol)	a (°A)	V(cm^3)	d_x(g/cm^3)
0.0	2.502	311	234.402	8.296	$5.709*10^{-22}$	5.440
0.3	2.501	311	234.450	8.293	$5.703*10^{-22}$	5.471
0.5	2.496	311	234.498	8.276	$5.668*10^{-22}$	5.496

3-Scanning Electron Microscopy (SEM)

In addition to atomic forcemicroscopy, scanning electron microscopy was carried out for further characterization of the morphology properties. The images in fig.4 showed not closely packed and consist of several grains and agree with[5].These micrographs exhibit the inhomogeneous grain size distribution.

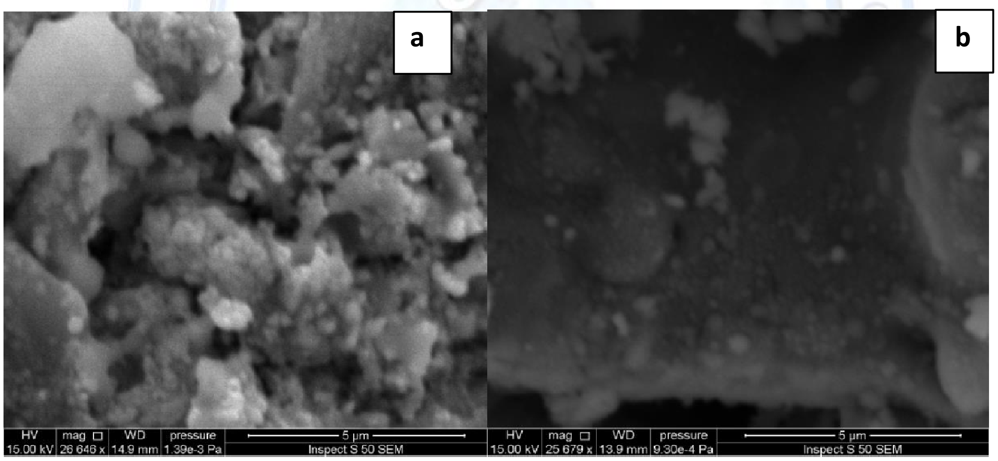

Fig (4) SEM images for bulk (a) $Ni_{0.7}Co_{0.3}Fe_2O_4$ and (b) $Ni_{0.5}Co_{0.5}Fe_2O_4$with 600 °C sintering temperature.

4-Compositionaland Frequency dependence of dielectric behavior

Figures (5 and 6) show the real part ofdielectric constant for samples prepared of ($Ni_{1-x}Cu_xFe_2O_4$) where (x=0.3 and 0.5) for different sample sintering temperatures as a function of frequency range from 50 KHz to 50 MHz.

The real part ofdielectric constant decreased with increasing frequency and reaches a constant value for all sample sintering temperatures[8,9]. The addition of copper generally enhances thereal part of dielectric constant values. However, the rate of decrease of the real part ofdielectric constant with frequency is slower with these additives.

The sintering temperature at which the sample shows the best real part ofdielectric constant is different for different copper additives. This can be explained by that two competitive process are exist; the first is the electron hopping between Fe^{2+} and Fe^{3+} ions and space charge polarization due to the presence of an inhomogeneous dielectric structure.The values of dielectric constant are high at low frequency and then decreases rapidly with the rise in frequency will be hindered i.e. the polarization decreases. Consequently, dielectric constant decreases with copper contents. Ultimately, it attains a constant value which is the general trend for all the ferrite samples [10].

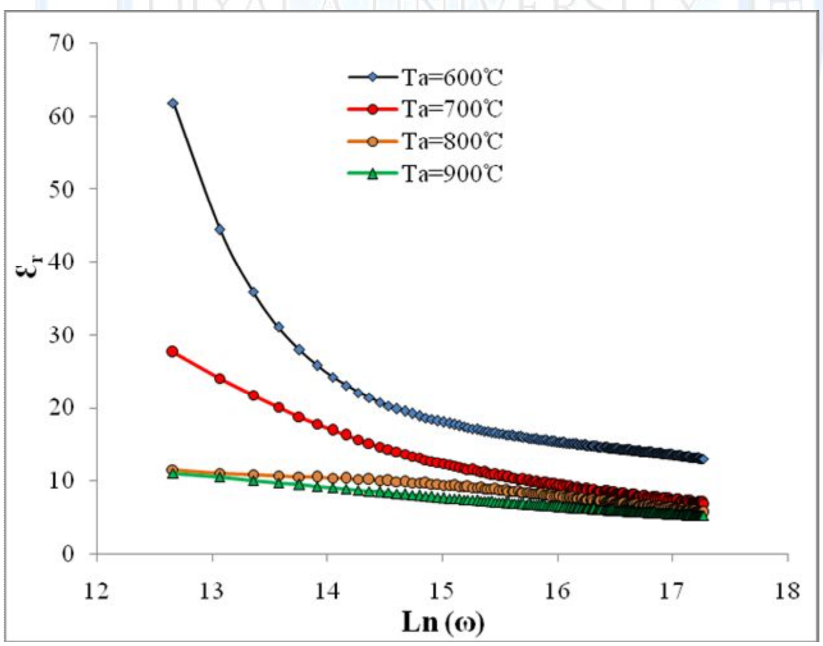

Fig.5 Change of real part of dielectric constant for bulk ($Ni_{0.7}Co_{0.3}Fe_2O_4$) with frequency and different sintering temperatures.

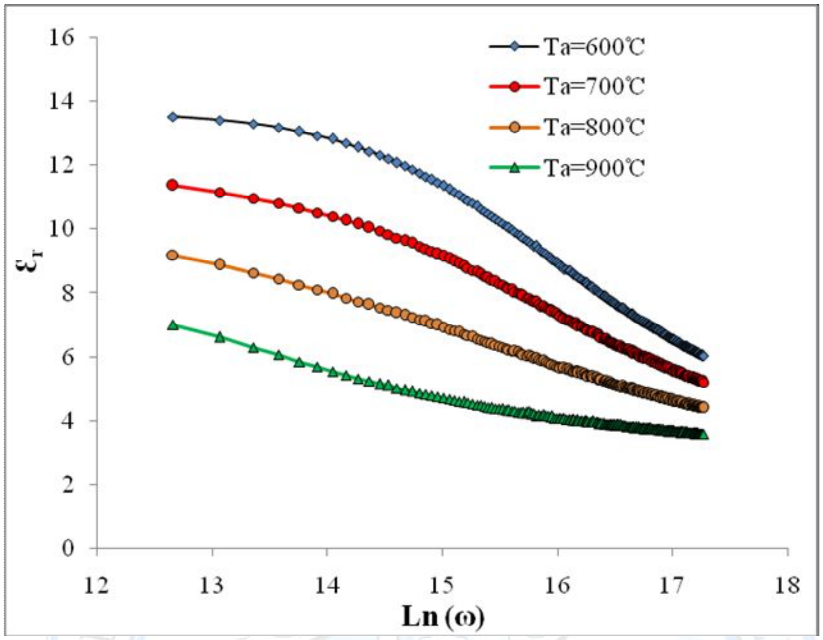

Fig.6 Change of real partof dielectric constant for bulk ($Ni_{0.5}Co_{0.5}Fe_2O_4$) with frequency and different sintering temperatures.

Figures (7and 8) showsimaginary part of dielectric constantversus frequency for the prepared samples at different sintering temperatures. The sintered shows decrease losses with high sintering temperature which may be explained by the evolution of free crystalline copperalong with ferrite burning. But, a low dielectric loss may be accompanied with low dielectric constant.

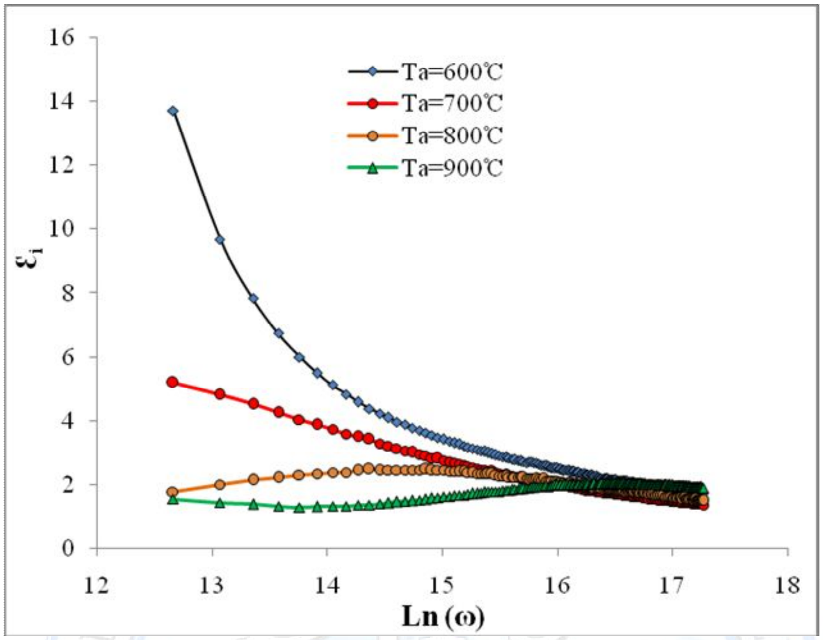

Fig. 7Changes of imaginary part of dielectric constant with frequency for bulk ($Ni_{0.7}Co_{0.3}Fe_2O_4$) with frequency and different sintering temperatures.

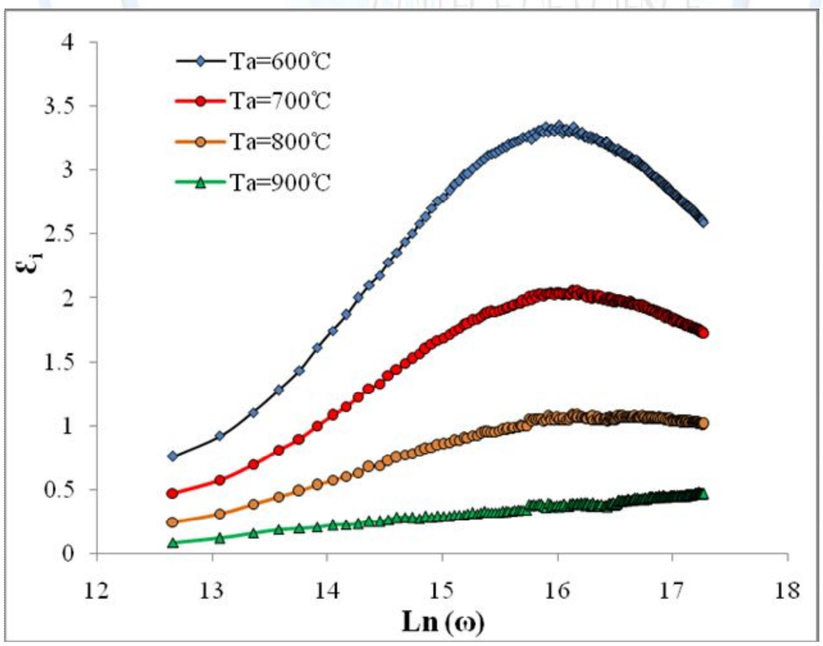

Fig.8 Changes of imaginary part of dielectric constant with frequency for bulk ($Ni_{0.5}Co_{0.5}Fe_2O_4$) with frequency and different sintering temperatures.

5-Relationship between conductivity and frequency

The $\sigma_{a.c}$ (ω)for ferrite ($Ni_{1-x}Cu_xFe_2O_4$) where (x=0.3 and 0.5) of copper additions and sintering at (600, 700, 800 and 900°C) for (2h)was found to increase with increasing the frequency according to empirical formula: $\sigma_{a.c}(\omega) = A\ \omega^s$[11,12]and with increasing concentration of copper as shown in figs (9 and 10) respectively. In this case, $\sigma_{a.c}$ (ω) is proportional to (ω^s) which means that $\sigma_{a.c}$ (ω) dominates at higher frequency in the range (50kHz to 5MHz). The conduction in ferrite is attributed to hopping of electrons from Fe^{3+} to Fe^{2+} ions. The number of such ion pairs depends upon the sintering temperature and the amount of reduction of Fe^{3+} to Fe^{2+} .For lower frequency in the range (50Hz to 50kHz) $\sigma_{a.c}(\omega)$ becomes independent of the frequency because D.C conductivity dominate in this frequency range .

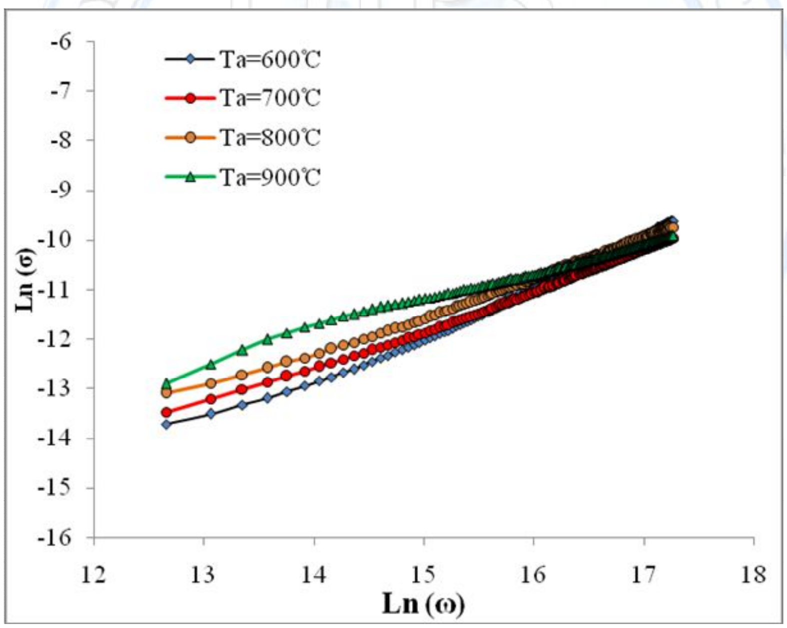

Fig.9 A.C conductivity as a function of frequency for bulk ($Ni_{0.7}Co_{0.3}Fe_2O_4$) with different sintering temperatures.

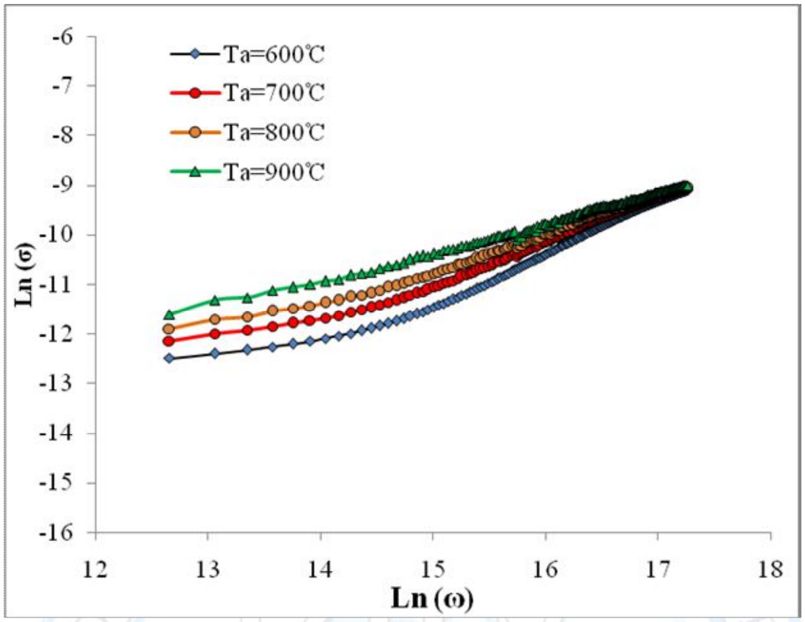

Fig.10 A.C conductivity as a function of frequency for bulk ($Ni_{0.5}Co_{0.5}Fe_2O_4$) with different sintering temperatures.

The values of exponent (s) for bulk ($Ni_{1-x}Cu_xFe_2O_4$) where (x=0.3 and 0.5) were estimated from the slope of the curves plotted between Ln $\sigma_{a.c}$ (ω) versus Ln(ω) as shown in Figs (9 and 10) which found to be less than unity for all prepared specimens which corresponding to correlated barrier model. Fig.(11) shows the value of exponent (s) with different sintering temperatures.

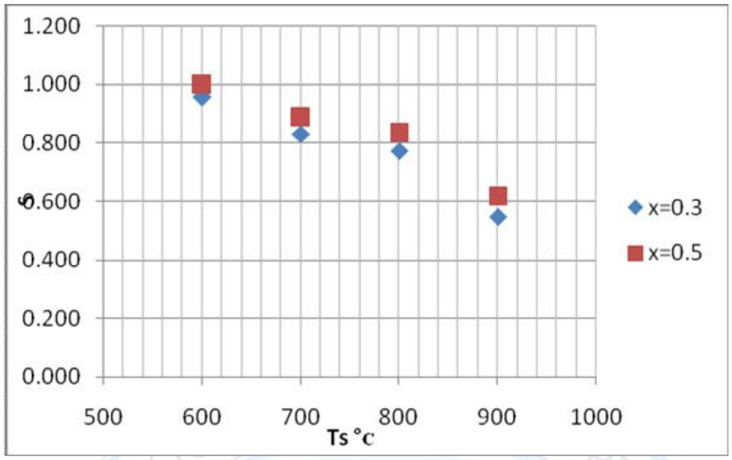

Fig.11 S- value as a function of different content of Cu for bulk ($Ni_{1-x}Cu_xFe_2O_4$) and different sintering temperatures.

Conclusion

Sol-gel method has been used to synthesize Cu substituted nickel ferrite samples at nanometer scale. Nickel ferrite ($NiFe_3O_4$) is prepared by employing hydrothermal sol gel technique. XRD studies reveals that the percentage of iron ions in B site increases with the reduction in grain size. This shifting of ions causes changes in XRD pattern also. As the percentage of iron ions in B site increases, the intensity of the (311) peak compared to that of the (220) peak increases. From the SEM image, it is observed that the granular size increases with increase in percentage of Ni and sintering temperature. The copper nickel ferrite shows high conductivity due to attribution of the dipole polarization. The high value of dielectric constant of the sample $Ni_XFe_{X-1}O_4$ is because of structural changes associated with the nickel ferrite when the grain size is reduced to nanometer order.

Reference

1. J.F.kennedy"*Future Ferrites and their Applications Huth III* ", Coil Winding 1986.
2. E.C. Butterworth, 'Soft Ferrites Properties and Applications, 2nd Edition Snelling'1988.
3. Lanlin Zha , The Ohio State University, R.Valenzuela, Magnetic Ceramics, Cambridge University press, Cambridge,2006.
4. M.A.Khan," *Fabrication and Characterization of Terbium Substituted Ferrites*",ph.D thesis, University Multan – Pakistan , 2011.
5. S. Ghatak, G. Chakraborty1, M.Sinha, S. K.Pradhan, and A. K.Meikap,"*Direct and Alternate Current Conductivity and Magnetoconductivity of Nanocrystalline Cadmium-Zinc Ferrite below Room Temperature* ", Materials Sciences and Applications, Vol.2,2011,pp. 226-236
6. A.M.Bhavikatti , S.Kulkarni , and A. Lagashetty, International journal of Engineering and Technology ,Vol.3 , No.1, 2011,pp.687-695 .
7. S.Sindhu, " *Preparation and Characterization of Spinel Ferrites - their Incorporation in Rubber Matrix and Evaluation of Properties* Cochin", University of Science and Technology, 2001.
8. F.L.Zabotto , A.J.Gualdi , J.A.Eiras , A.J.A. Oliveira and D. Garcia , Material Research , Vol.15, No.3,pp. 428-433, 2012.
9. J.P.Mallick, " *A Comparative Study of the Structure & Magnetic Properties of Nickel Cobalt Ferrites Synthesized by Solid State & Auto-Combustion Processing Techniques*" , B.Sc thesis, National Institute of Technology , 2011.
10. S. Ghatak, G. Chakraborty1, M.Sinha, S. K.Pradhan, and A. K.Meikap, Materials Sciences and Applications, Vol.2,pp. 226-236, 2011.
11. P.A. Noorkhan and S. Kalayne ,International Journal of Modern Engineering Research, Vol.2, Issue.4,2012, pp-2303-2306.
12. Y. L. N Murthy, I .V K.Viswanath, T. K. Rao, and R. singh, International Journal of ChemTech Research ,Vol.1,No.4, pp. 1308-1311, 2009 .